Available online at www.sciencedirect.com
SCIENCE DIRECT®
ELSEVIER
Ultramicroscopy 99 (2004) 179–187
ultramicroscopy
www.elsevier.com/locate/ultramic

Optimal resolution of a time-dependent aberrationless magnetic lens

M. Calvo

Instituto de Física, Universidad Católica de Valparaíso, P.O. Box 4059, Valparaíso, Chile

Received 24 March 2003; received in revised form 10 January 2004; accepted 26 January 2004

Abstract

We analyse the optimal conditions for operation of a time-dependent magnetic field lens recently proposed. The lens consists of an axially symmetric ellipsoidal coil producing a spatially homogeneous but time-pulsating magnetic field. This system is capable of focusing a beam of charged particles drifting parallel to the coil axis as well as forming images of an object emitting electrons. This lens has no spherical aberration and, consequently, opens the possibility of surpassing the resolving power of conventional round static field lenses. The cardinal elements of this lens are functions of time and thereby the image position, its magnification factor and orientation change in time. We show how by a suitable choice of the magnetic field pulse parameters and the introduction of screens with circular apertures, it is possible to render all the image characteristics stationary. The effect of diffraction is also discussed in the context of transfer function theory.

PACS: 07.78 + s; 41.85P; 41.85Gy

Keywords: Aberrationless magnetic lenses

The aim of designing an electron lens free of aberrations has been a challenge for electron microscopist ever since the first microscopes were built. For years scientists analyzed different types of lenses with the hope of constructing the perfect lens. In 1940 Scherzer, in a celebrated theorem [1], proved that for a general class of axially symmetric static field lenses the geometrical aberrations impose a theoretical resolution limit which cannot be surpassed. A way of avoiding the implications of this theorem is to include multipole nonsymmetric lenses, electron mirrors and time-dependent fields, among the most important [2]. Multipole fields have been incorporated successfully by correcting order by order the aberrations of a conventional lens [3]. In a similar approach, time-dependent fields have been proposed by coupling a microwave cavity to a static lens [4]. The central idea is to correct the aberrations of the lens by employing pulsed beams properly tuned with the cavity fields. Although simple in principle, this technique imposes very stringent conditions on the cavity fields which are very difficult to meet experimentally.

In this work we describe the theory of a new type of lens based on a different principle, which employs a space uniform but time pulsating magnetic field together with the induced axially

E-mail address: mcalvo@ucv.cl (M. Calvo).

0304-3991/$ - see front matter © 2004 Published by Elsevier B.V.
doi:10.1016/j.ultramic.2004.01.001

symmetric electric field. By analyzing the electrons trajectories we will find that this system can focus a beam of parallel electrons incident upon the field region along the symmetry axis or that it can form an image of some object emitting electrons. A detailed account of these properties have been published elsewhere and, therefore, we will briefly outline them here [5,6]. Our main goal in this work is to analyze the operational conditions under which, with the exception of diffraction, all forms of aberrations are, at least in principle, eliminated. The lens in question consists of an axially symmetric ellipsoidally shaped coil for which the number of turns per unit axial length is fixed. Such coils are known for producing a space uniform internal magnetic field and for this reason they are employed in certain mass spectrometers having this requirement. If a current source of controllable intensity, $I(t)$, is connected to the coil a magnetic field proportional to $I(t)$ is produced. Except for extremely rapid changing currents the resulting field is well approximated by the space-independent magnetostatic expression and the resulting induced electric field by Faraday's law. Departures from magnetic field space homogeneity inside the coil can be estimated in a simple way and, as a general rule, it can be shown that provided the characteristic time of variation of $I(t)$ is much larger that the time light takes to cross a distance comparable to the electrons beam diameter, this approximation is well justified. See appendix.

Let us assume that the coil axis is oriented along the z-axis so that the magnetic field is given by $\mathbf{B}(t) = B(t)\hat{z}$ and the resulting electric field is $\mathbf{E}(\mathbf{r}, t) = \mathbf{r} \times \dot{\mathbf{B}}(t)/2c$, where the dot indicates time derivative. We note that these expressions must be modified at the coil tips for which fringing field effects take place. Clearly, the resulting Lorentz force only acts on the x–y plane and thus the motion along the z-axis consists of a free drift with constant momentum mv_z^0. Ignoring temporarily fringe field effects and assuming non-relativistic motion, the equation of motion is

$$\ddot{\vec{r}}(t) + \dot{\vec{r}}(t) \times \vec{\omega} + \tfrac{1}{2}\vec{r}(t) \times \dot{\vec{\omega}} = 0, \quad (1)$$

where $\boldsymbol{\omega} = (eB(t)/mc)\hat{z}$ and $\mathbf{r}$ represents the electron transverse position. The general solution satisfying the initial conditions $\mathbf{r}(t_0) = \mathbf{r}_{\text{in}}, \dot{\mathbf{r}}(t_0) = \mathbf{v}_{\text{in}}$ can be written as

$$\mathbf{r}(t, t_0) = \mathbf{R}\left[\frac{\theta(t, t_0)}{2}\right]\Big[u_1(t, t_0)\mathbf{v}_{\text{in}} + u_2(t, t_0)\mathbf{r}_{\text{in}} - \frac{1}{2}u_1(t, t_0)(\omega(t_0) \times \mathbf{r}_{\text{in}})\Big], \quad (2)$$

where $u_{1,2}(t; t_0)$ are two particular solutions of

$$\ddot{u}(t) + \left(\frac{\omega(t)}{2}\right)^2 u(t) = 0 \quad (3)$$

satisfying the following initial conditions: $u_1(t_0, t_0) = \dot{u}_2(t_0, t_0) = 0, \dot{u}_1(t_0, t_0) = u_2(t_0, t_0) = 1$ and

$$R\left(\frac{\theta}{2}\right) = \begin{bmatrix} \cos\theta/2 & -\sin\theta/2 \\ \sin\theta/2 & \cos\theta/2 \end{bmatrix}, \quad (4)$$

with $\theta(t, t_0) = \int_{t_0}^{t} \mathrm{d}t'\omega(t')$. In this form, the problem of determining the electrons trajectories is reduced to finding the solutions $u_{1,2}(t, t_0)$.

Let us note some general properties of Eq. (2). First if $v_{\text{in}} = 0$ and $\omega(t_0) = 0$, then every time t_2 for which $u_2(t_2) = 0$, and irrespective of $\mathbf{r}_{\text{in}}, \mathbf{r}(t_2) = 0$. On the other hand, for every t_1 for which $u_1(t_1) = 0$, Eq. (2) yields

$$\mathbf{r}(t_1) = \Re\left[\frac{\theta(t_1, t_0)}{2}\right]u_2(t_1)\mathbf{r}_{\text{in}}, \quad (5)$$

which implies that, irrespective of v_{in}, the position at t_1 is obtained from $\mathbf{r}_{\text{in}}$ by a rotation by $\theta(t_1)/2$ and rescaling by $u_2(t_1)$ (in fact the whole transverse configuration space is rotated and rescaled). These two properties constitute, respectively, the basis for beam focusing and image formation of our system. Let us note that for a given $\omega(t)$, a different choice of t_0, say t_0', will, in general, yield different functions $u_{1,2}(t)$, different t_1', t_2' and different $t_1 - t_0, t_1' - t_0'$ or $t_2 - t_0, t_2' - t_0'$. If we imagine a beam of particles initially travelling parallel to the z-axis and entering the solenoid at t_0, at time t_2 they will be focused. By the same token, particles emitted by some object at t_0, will form an image at t_1 according to Eq. (4). The focusing or object–image distances are $(t_2 - t_0)v_d^0$ and $(t_1 - t_0)v_d^0$, respectively. Consequently, for a continuous beam the position of the focus as well as the distance, the scale and the rotation of the image will be changing in time. To obtain a stationary focusing or image, short particle pulses must be employed. In addition, in order to reduce the aberrations resulting from this time dependence, the choice of the pulse injection times as well as other features of the field $\omega(t)$ must be chosen appropriately so that the beam focusing remains temporary stationary.

Let us assume the magnetic field has the form depicted in Fig. 1. The electrons pulse is emitted by the object during the time interval $[\tilde{t}_0, \tilde{t}_0 + \Delta t]$, where Δt is the pulse duration and $\tilde{t}_0$ the instant the emission initiates. Since the magnetic field vanishes during this interval, we conclude from Eq. (3) and the initial conditions $u_2(t_0, t_0) = 1$, $\dot{u}_2(t_0, t_0) = 0$ with $\tilde{t}_0 \leqslant t_0 \leqslant \tilde{t}_0 + \Delta t$, that

$$u_2(t, t_0) \equiv u_2(t, t_0') \tag{6}$$

for any pair t_0, t_0' within this interval. (Actually this is valid for any t_0, t_0' inside the interval $[\tilde{t}_0, T_{\rm on}]$ where $T_{\rm on}$ is the time the magnetic field starts to build up.) Moreover, we also note that for $t > T_{\rm off}$, with $T_{\rm off}$ being the time the field is switched off, the resulting function $u_2(t, t_0)$ will be a linear function of t. Let us assume that we shape the magnetic pulse such that $\dot{u}_2(T_{\rm off}; t_0) = 0$ and $|u_2(T_{\rm off}; t_0)| \neq 1$. This latter requirement guarantees that we have a magnified ($|u_2| > 1$) or demagnified ($|u_2| < 1$) image. The importance of the condition $u_2(t, t_0) = \text{constant}$ for $t > T_{\rm off}$ is that the image magnification factor will be the same for <u>all</u> electrons in the pulse, irrespective of their emission time t_0. On the other hand, the form of the function $u_1(t, t_0)$ will change with t_0 and, consequently, the image formation time t_1, determined from $u_1(t_1, t_0) = 0$, will depend on t_0 and, in addition, $t_1 - t_0 \neq t_1' - t_0'$ for $t_0 \neq t_0'$. We assume that the magnetic field shape is such that $t_1' > T_{\rm off}$ for all t_0'. Accordingly, the functions $u_1(t, t_0')$ will be linear functions of t for $t > T_{\rm off}$,

$$u_1(t, t_0') = (t - T_{\rm off})\dot{u}_1(T_{\rm off}, t_0') + u_1(T_{\rm off}, t_0'), \tag{7}$$

where t_1' is determined by

$$t_1' = T_{\rm off} - u_1(T_{\rm off}, t_0')/\dot{u}_1(T_{\rm off}, t_0'). \tag{8}$$

Consequently, the choice of magnetic field must be such that

$$u_1(T_{\rm off}, t_0')/\dot{u}_1(T_{\rm off}, t_0') < 0 \tag{9}$$

for all t_0'. This property guarantees that the rotation angle of the image relative to the object

$$\theta(t_1', t_0') = \int_{t_0'}^{t_1'} \omega(\bar{t})\, d\bar{t}$$

is the same for all electrons in the pulse. Finally we note that the image–object distance, given by $(t_1' - t_0')v_z^0 = d(t_0')$ will depend on t_0' and, consequently, superimposing the images formed by the distinct electrons of the pulse at some fixed distance from the object will produce a defocusing aberration. In conclusion, we have shown how electrons within a finite pulse form images which have the same amplification, the same rotation angle, but are focused at different planes.

So far in this analysis we have assumed a monochromatic beam so that all electrons come with the same axial velocity v_z^0. Evidently, this condition will never be met in practice and, therefore, we must also take this effect into account. Clearly, a dispersion in v_z^0 will affect the position of the images since slower or faster electrons, although emitted simultaneously, will form images closer or farther away from the object. Consequently, this form of (chromatic) aberration will have the same defocusing effect on the image recording process as the finite electron pulse duration. In the following, we will show how it is possible to virtually eliminate both effects. To obtain this, we begin by introducing one aperture along the lens axis which only allows unscattered electrons that emerged from the object with $\mathbf{v}_{\rm in} = 0$. This is achieved by inserting a screen with a small circular aperture centered at the z-axis and located downstream at a distance $v_z^0(t_2 - t_0)$ from the object. As we showed before, at this instant all electron ejected by the object at t_0 with $\mathbf{v}_{\rm in} = 0$ are focused at a distance $(t_2 - t_0)v_z^0$ from the object. In addition, we note that electrons in the pulse emitted at $t_0' \neq t_0$ will also focus at t_2 but their focal distance, $(t_2 - t_0')v_z^0$, will differ from $(t_2 - t_0)v_z^0$ and, consequently, will be intersected by the screen. Finally, we note that electrons emitted at t_0 but with $v_z \neq v_z^0$, are also absorbed because of their different focal distance. We note that there will be some fraction of the electrons, emitted at some $t_0' \neq t_0$, with $v_z \neq v_z^0$, but such that

$(t_2 - t'_0)v_z = (t_2 - t_0)v_z^0$. Clearly these reach the screen focal point at t_2 and will not be filtered. In order to eliminate these unwanted electrons without affecting the rest, we will introduce a second screen identical to the first but located further downstream along the lens axis at a distance $(t'_2 - t_0)v_z^0$ from the object, where t'_2 is another zero of the function $u_2(t'_2, t_0) = 0$. Evidently this latter screen will only intersect those electrons which managed to go through the first screen with $v_z \neq v_z^0$, since they will be focused at a distance $(t'_2 - t_2)v_z$ from the first screen, which differs from the selected distance between both screens $(t'_2 - t_2)v_z^0$. The particular choice of t_0 within the interval $\tilde{t}_0 \leqslant t_0 \leqslant \tilde{t}_0 + \Delta t$ will depend on the local electron current density along the pulse and can be chosen so as to maximize the fraction of unfiltered electrons. In conclusion, this screens system acts as a monochromator but, in addition, it selects from a finite electron pulse only those ejected by the object at some conveniently chosen instant t_0, and consequently chromatic and finite pulse aberrations can be eliminated.

The finite diameters of the screens holes will produce aberrations which we will evaluate below. Clearly, the first aperture will allow electrons within some range $t_0 \pm \delta t_0$ of the full pulse to go through it and, similarly, the second screen will permit electrons with some axial velocity dispersion δv_z. Both δv_z and δt_0 are functions of the holes diameters $d_{1,2}$, and produce aberrations at the image plane. We showed above how electrons with $\mathbf{v}_{\text{in}} = 0$, the same v_z and emitted either at t_0 or $t_0 + \delta t_0$ will focus at t_2. However, an electron emitted at $t_0 + \delta t_0$ will have a different focal distance. Clearly, it will reach the first screen at time $t_2 + \delta t_0$ and, therefore, it will go through it only if

$$|\mathbf{r}(t_2 + \delta t_0, t_0 + \delta t_0)| < d_1. \tag{10}$$

It then follows from Eq. (2) that

$$\begin{aligned} &|\mathbf{r}(t_2 + \delta t_0, t_0 + \delta t_0)| \\ &\quad = |u_1(t_2 + \delta t_0, t_0 + \delta t_0)\mathbf{v}_{\text{in}} + u_2(t_2 + \delta t_0, t_0)\mathbf{r}_{\text{in}}| \\ &\quad \simeq |(u_1(t_2, t_0) + \dot{u}_1(t_2, t_0)\delta t_0)\mathbf{v}_{\text{in}} \\ &\qquad + \dot{u}_2(t_2, t_0)\delta t_0 \mathbf{r}_{\text{in}}|, \end{aligned} \tag{11}$$

where we have expanded the functions the functions $u_{1,2}$ to order δt_0 and recalled that $u_2(t_2, t_0) = 0$. An estimate of the maximal $\mathbf{v}_{\text{in}}$ is obtained by setting $\delta t_0 = 0$

$$|\mathbf{v}_{\text{in}}| \leqslant d_1 / |u_1(t_2, t_0)| \tag{12}$$

(we note that electrons emitted at t_0 with $\mathbf{v}_{\text{in}} \neq 0$ produce no image aberrations). Similarly, the maximum δt_0 occurs for $v_{\text{in}} = 0$ and is

$$\delta t_0 = \frac{d_0}{|\dot{u}_2(t_2, t_0)\mathbf{r}_{\text{in}}|}. \tag{13}$$

Evidently $|\mathbf{r}_{\text{in}}|$ will depend on the point within the image, however, let us assume that the object is located at some radial distance $\gg d_1$ from the z axis so that $d_1/\mathbf{r}_{\text{in}}| \ll 1$ for all points of the object (for example, $d_1 \simeq 2\ \mu\text{m}$ and $|\mathbf{r}_{\text{in}}| \simeq 2\ \text{mm}$ yield $d_1/|\mathbf{r}_{\text{in}}| \simeq 10^{-3}$). In this case we obtain

$$\delta t_0 \simeq \frac{d_1}{|\mathbf{r}_{\text{in}}|} \frac{1}{|\dot{u}_2(t_2, t_0)|} = \frac{d_1}{r_{\text{in}}} |u_1(t_2, t_0)|. \tag{14}$$

Consequently, the aberration at the image resulting from δt_0 is

$$\begin{aligned} |\Delta \mathbf{r}| &= |\mathbf{r}(t_1 + \delta t_0, t_0 + \delta t_0) - \mathbf{r}(t_1, t_0)| \\ &= \left| \left(u_2(t_1, t_0) - \frac{1}{u_2(t_1, t_0)} \right) \mathbf{v}_{\text{in}} \delta t_0 \right| \\ &= |u_2(t_1, t_0) - 1/u_2(t_1, t_0)| \frac{d_1^2}{\langle r_{\text{in}} \rangle}, \end{aligned} \tag{15}$$

where we used $\dot{u}_2(t_1, t_0) = 0$ and $\langle r_{\text{in}} \rangle$ represents the mean radial distance of the object. Assuming the amplification factor is $u_2(t_1, t_0) \sim 10^4$ and $d_1/\langle r_{\text{in}} \rangle \sim 10^{-3}$ we derive $|\Delta \mathbf{r}| \simeq 10^{-3}$ cm, which is in the range of resolution of a recording fluorescent screen or photographic plate. On the other hand, we can estimate δt_0 from Eq. (13) by assuming $\dot{u}_2(t_2, t_0) \sim \bar{\omega}$ where $\bar{\omega} = e\bar{B}/mc$ with $\bar{B}$ the mean strength of the coil magnetic field. Thus if $B_0 \sim 10-10^2$ G, $\bar{\omega} \sim 10^9\ \text{s}^{-1}$ and $\delta t_0 \sim 10^{-12}-10^{-13}$ s.

Chromatic aberration resulting from the dispersion δv_z can be estimated by noting that an electron with axial velocity $v_z^0 + \delta v_z$, which crossed the first screen aperture at t_2, will reach the second aperture at time t given by

$$(t - t_2)(v_z^0 + \delta v_z) = D = (t'_2 - t_2)v_z^0, \tag{16}$$

with D being the distance separating the screens. Thus if we call

$$\Delta t = t - t_2' = \frac{\delta v_z}{v_z^0}(t_2' - t_2),$$

this electron will go through the second screen provided

$$d_2 \geqslant |\mathbf{r}(t_2' + \Delta t, t_0)| = |u_1(t_2', t_0)\mathbf{v}_{\text{in}} + \dot{u}_2(t_2', t_0)\Delta t\,\mathbf{r}_{\text{in}}|. \tag{17}$$

This expression yields an estimate of the largest Δt or $\delta v_z/v_z^0$

$$\frac{\delta v_z}{v_z^0} \simeq \frac{d_2}{r_{\text{in}}}\frac{u_1(t_2', t_0)}{(t_2' - t_2)}. \tag{18}$$

This electron will reach the image plane in a time interval $t_1 + \overline{\Delta t} - t_0$ given by

$$(v_z^0 + \delta v_z)(t_1 + \overline{\Delta t} - t_0) = v_z^0(t_1 - t_0), \tag{19}$$

so that

$$\overline{\Delta t} = \frac{\delta v_z}{v_z^0}(t_1 - t_0). \tag{20}$$

Therefore, the aberration resulting from the velocity dispersion becomes

$$\begin{aligned} |\Delta\mathbf{r}| &= |\mathbf{r}(t_1 + \overline{\Delta t}, t_0) - \mathbf{r}(t_1, t_0)| \simeq |\dot{u}_2(t_1, t_0)\mathbf{r}_{\text{in}}\overline{\Delta t}| \\ &= |\dot{u}_2(t_1, t_0)|d_2|u_1(t_2', t_0)|\frac{t_1 - t_0}{t_2 - t_2'} \\ &= \left|\frac{\dot{u}_2(t_1, t_0)(t_1 - t_0)}{\dot{u}_2(t_2, t_0)(t_2' - t_2)}\right| d_2. \end{aligned} \tag{21}$$

The last factor will depend on the particular form of the magnetic field. In a recent publication [6], we analyzed the case of a compound pulse consisting of a magnetic field of constant strength B_0 acting during a time interval τ_0, followed by another pulse of similar characteristics but of strength B_1 and duration τ_1. In Fig. 1 we depict the profile of this sequence. It was found that in this case the resulting amplification factor was rather modest $u_2(t_1) \simeq \sqrt{2}$. Therefore, in order to gain a more significant amplification this compound pulse was iterated in such a way that the first image becomes the object of the second pulses and so on. In this way, we found that after a series of 32 such pulses the resulting amplification factor, become $(\sqrt{2})^{32} \simeq 6.6 \times 10^4$. Evidently, during this time lapse the resulting functions $u_1(t), u_2(t)$ have a

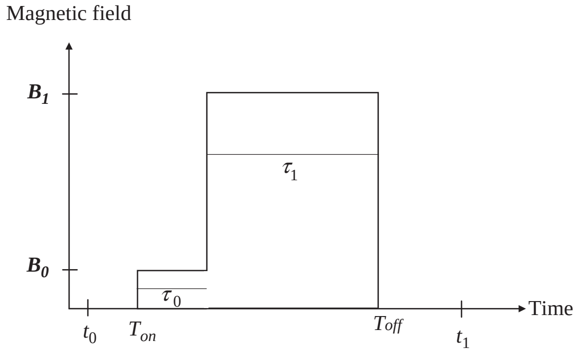

Fig. 1. Magnetic field profile for an asymmetric magnetic pulse. Electrons are ejected by the object at $t_0 = 0$ and enter into the coil. At time T_{on} a magnetic field of strength B_0 is turned on for a time interval τ_0, followed by a field of strength B_1 which acts for a time interval τ_1. At time T_{off} the field is turned off and electrons form an image at time t_1. In our example and to simplify the mathematics we have assumed instantaneous grow of the field. In a real experiment the field will evidently grow or decrease continuously from one value to the next.

series of alternating zeroes. Therefore, we have multiple choices for t_2 and t_2' or, equivalently, for the positions of the filtering screens described above. If we chose, for example, the first and the last zeroes of $u_2(t)$ for t_2 and t_2' respectively, it follows from our previous analysis that the ratio

$$\left|\frac{\dot{u}_2(t_1, t_0)(t_1 - t_0)}{\dot{u}_2(t_2, t_0)(t_2' - t_0)}\right| \simeq 1, \tag{22}$$

so that chromatic aberration at the image plane will, in this case, be $|\Delta\mathbf{r}| \sim d_2 = 10^{-4}$ cm.

So far we have ignored in our analysis diffraction. It is evident that the apertures introduced above will produce diffraction. The smaller the diameters of the apertures the more effective the screen system becomes in reducing aberrations (Eq. (15,21)). On the other hand, too small apertures will enhance diffraction and, in addition, will eventually reduce the electron current beyond some minimal desirable threshold necessary for image detection. In consequence, some compromise must be taken between these two competing effects. A simple analysis based on the Airy pattern of diffraction produced by the second screen aperture yields a diffraction aberration radius

$$|\Delta\mathbf{r}_{\text{d}}| \simeq \lambda(t_1 - t_2)v_z^0/d_2, \tag{23}$$

where λ is the electron wave length and $(t_1 - t_2)v_z^0$ represents the distance screen-image. If we assume $\lambda \sim 10^{-9}$ cm, $(t_i - t_2)v_z^0 \sim 10$ cm and $d_2 \sim 10^{-4}$ cm, we obtain $|\Delta \mathbf{r}_\mathrm{d}| \sim 10^{-5}$ cm, indicating that for this range of parameters diffraction is 10 times smaller than the previous form of aberration.

We will finally develop the wave mechanical theory to treat the electrons evolution through the system [7] . This analysis is based on the transfer functions theory and a detailed description have been published elsewhere [8]. The main idea is to construct the propagator for the electrons leaving the object plane, going through the lens with its apertures, and ending at the image recording plane. The solution to this problem is conveniently obtained in terms of the propagator function $\tilde{G}(\mathbf{r}, z, t; r', z', t_0)$ satisfying:

$$\left(\mathrm{i}\hbar\frac{\partial}{\partial t} - H\right)\tilde{G} = \mathrm{i}\hbar\delta(z - z')\delta^2(\mathbf{r} - \mathbf{r}')\delta(t - t_0), \quad (24)$$

where

$$H = \left(\mathbf{P} + \frac{e}{c}\mathbf{A}\right)^2/2m = \left(\mathbf{P}_t + \frac{e}{c}\mathbf{A}(\mathbf{r}, t)\right)^2/2m + P_z^2/2m$$

with

$$\mathbf{A}(\mathbf{r}, t) = (\mathbf{r} \times \mathbf{B}(t))/2. \quad (25)$$

Since the motion along the z-axis is decoupled from the transverse motion, the propagator can be factorized as a product

$$\tilde{G}(\mathbf{r}, z, t; \mathbf{r}', z', t_0) = G(r, t; \mathbf{r}', t_0)g(z, t; z', t_0), \quad (26)$$

where $g(z, t; z', t_0)$ is the one-dimensional free particle propagator

$$g(z, t; z', t_0) = (m/2\pi\mathrm{i}\hbar(t - t_0))^{1/2} \times \exp\left\{\frac{\mathrm{i}m(z - z')^2}{2\hbar(t - t_0)}\right\} \quad (27)$$

and $G(\mathbf{r}, t; \mathbf{r}', t_0)$ is a solution of

$$\left[\mathrm{i}\hbar\frac{\partial}{\partial t} - \left(\vec{P}_t + \frac{e}{c}\mathbf{A}\right)^2/2m\right]G(\mathbf{r}, t; \mathbf{r}', t') = \mathrm{i}\hbar\delta^2(\mathbf{r} - \mathbf{r}')\delta(t - t_0), \quad (28)$$

representing the propagation in the xy plane. The solution for $G(\mathbf{r}, t; \mathbf{r}', t_0)$ is readily expressed in terms of the functions $u_1(t, t_0), u_2(t, t_0)$ derived before and is given by

$$G(\mathbf{r}, t; \mathbf{r}', t_0) = (m/2\pi\mathrm{i}\hbar u_1(t, t_0)) \exp\frac{\mathrm{i}m}{2\hbar u_1(t, t_0)} \times \left[\dot{u}_1(t, t_0)r^2 + u_2(t, t_0)r'^2 - 2\mathbf{r}\cdot R\left(\frac{\theta(t, t_0)}{2}\right)\mathbf{r}'\right]. \quad (29)$$

It is easily checked that

$$\lim_{t \to t_0} G(\mathbf{r}, t, \mathbf{r}', t_0) = \delta^2(\mathbf{r} - \mathbf{r}') \quad (30)$$

as expected. Then the time evolved wave function is given by

$$\psi(\mathbf{r}, z, t) = \int\int G(\mathbf{r}, t; \mathbf{r}', t_0)g(z, t; z', t_0) \times \psi_0(\mathbf{r}', z', t_0)\,\mathrm{d}^2r'\,\mathrm{d}z'. \quad (31)$$

Let us suppose the initial wave function $\psi_0(\mathbf{r}', z', t_0)$ is factored into a product $\phi(\mathbf{r}', t_0)\chi(z', t_0)$, where $\chi(z', t_0)$ has the form of a wave packet with average momentum mv_z^0. In this case the evolution of ϕ and χ proceeds independently and we will focus in $\phi(\mathbf{r}, t)$.

$$\phi(\mathbf{r}, t) = \int G(\mathbf{r}, t; \mathbf{r}', t_0)\phi(\mathbf{r}', t_0)\,\mathrm{d}^2r'. \quad (32)$$

The complete evolution of the wave function through the system, will be divided into three steps. The evolution from the object to the first aperture, this is determined by Eq. (32) with $t = t_2$. At this point the effect of the screen is incorporated by multiplying the resulting wave function by some symmetric function $A(r)$. This function is unity for the open parts of the screen and zero for the opaque parts. Thereafter the resulting function is propagated to the second screen with t_2 and t_2' being, respectively, the intermediate initial and final times appearing in Eq. (32). The second screen is represented by a multiplicative screen function $A_2(r)$. Finally, the resulting function is time evolved to the image plane with t_2' and t_1 being, respectively, the initial and final times of the propagator during this last step. In conclusion, the resulting wave function is

$$\psi(\mathbf{r},t_1)=\int\int\int G(\mathbf{r},t_1;\mathbf{r}',t_2')A_2(r')G(\mathbf{r}',t_2';\mathbf{r}'',t_2)\times A_1(r'')G(\mathbf{r}'',t_2;\mathbf{r}''',t_0)$$

$$\psi(\mathbf{r}''',t_0)\,\mathrm{d}^2r'\,\mathrm{d}^2r''\,\mathrm{d}^2r'''. \tag{33}$$

Let $\tilde{\phi}(\mathbf{k},t)$ stand for the Fourier transform of $\psi(\mathbf{r},t)$ and assume the electron emerges from the object located at $z=0$, at t_0. The screens are located at positions $z_1=v_z^0(t_2-t_0)$. and $z_2=v_z^0(t_2'-t_0)$, respectively, and the image recording plane is at $z_i=v_z^0(t_1-t_0)$. If we substitute for the corresponding propagators in Eq. (33) and express them in terms of the functions $u_1(t),u_2(t)$ satisfying the initial conditions $u_1(t_0)=\dot{u}_2(t_0)=0$ and $\dot{u}_1(t_0)=u_2(t_0)=1$, we obtain after some straightforward algebra

$$\psi(\mathbf{r}_i,t_1)=\left(\frac{m}{\hbar}\right)^2\frac{1}{u_2(t_1)}\times\int\int\frac{\mathrm{d}^2r}{(2\pi)^2}\left\{A_2(u_1(t_2')r)A_1(u_1(t_2)r)\times\tilde{\phi}\left(\frac{m}{\hbar}R^{-1}\left(\frac{\theta(t_2,t_0)}{2}\right)\mathbf{r},t_0\right)\right\}\times\exp(\mathrm{i}\boldsymbol{\rho}\cdot\mathbf{r}), \tag{34}$$

where

$$\boldsymbol{\rho}=\frac{m}{\hbar}\frac{1}{u_2(t_1)}R^{-1}\left(\frac{\theta(t_1,t_2')}{2}\right)\mathbf{r}_i.$$

To derive this result we made use of the fact that $u_2(t_2)=u_2(t_2')=0$ and $u_1(t_i)=\dot{u}_2(t_i)=0$. If we Fourier transform Eq. (34), we derive

$$\tilde{\phi}(\mathbf{k},t_i)=u_2(t_i)A_2\left(\frac{\hbar}{m}u_2(t_1)u_1(t_2')k\right)A_1\left(\frac{\hbar}{m}u_2(t_1)u_1(t_2)k\right)\times\tilde{\phi}(u_2(t_1)R^{-1}(\theta(t_i,t_0))\mathbf{k},t_0). \tag{35}$$

This simple result shows that the lens-double screen system acts as a linear filter of the frequency spectrum of the Fourier transform of the object wavefunction. If the screens aperture functions have different diameters d_1,d_2, it is evident from Eq. (34) that the effective frequency cutoff will be determined by the screen with the smallest of $d_2/u_1(t_2')$, or $d_2/u_1(t_2)$ so that, in effect, for this electron only one screen is relevant.

Let us assume that the object consists of a thin specimen and that the incident electron wavefunction is a plane wave. The emerging wavefunction has the form

$$\psi(\mathbf{r},t_0)=(1-a(\mathbf{r}))\mathrm{e}^{\mathrm{i}\sigma(\mathbf{r})}\simeq1-a(\mathbf{r})+\mathrm{i}\sigma(\mathbf{r}) \tag{36}$$

with both $a(\mathbf{r})\ll1$ and $\sigma(\mathbf{r})\ll1$. In this case we find

$$\tilde{\phi}(\mathbf{k},t_0)=(2\pi)^2\delta^2(\mathbf{k})-\tilde{a}(k)+\mathrm{i}\tilde{\sigma}(\mathbf{k}),$$

where $\tilde{a}(\mathbf{k})$ and $\tilde{\sigma}(\mathbf{k})$ are the Fourier transform of $a(\mathbf{r})$ and $\sigma(\mathbf{r})$ respectively. Substituting it into Eq. (35) yields the Fourier transform the image wavefunction. Finally, inverting this Fourier transform and evaluating the image contrast function, defined as

$$1-(u_2(t_1))^2|\psi(\mathbf{r},t_1)|^2, \tag{37}$$

we obtain

$$1-(u_2(t_i))^2|\psi(\mathbf{r},t_i)|^2=2\int\frac{\mathrm{d}^2k}{(2\pi)^2}\tilde{a}(\mathbf{k})A_1\left(\frac{\hbar}{m}u_1(t_2)\mathbf{k}\right)\times\exp i(\mathbf{k}\cdot R^{-1}(\theta(t_i,t_0))\mathbf{r})/u_2(t_i), \tag{38}$$

where we assumed A_1 yields the lowest frequency cutoff, omitted A_2 in Eq. (35) and linearized the resulting expression in a and σ. This result indicates that in this case contrast arises entirely from the amplitude modulation function and is independent of the object phase function $\boldsymbol{\sigma}$.

Let us next analyze the evolution of the wavefunction for an electron emitted at $t_0+\Delta t$ and recorded at the image plane at $t_1+\Delta t$. We assume that this electron emerges with the same initial wavefunction as the preceding one, so that $\psi'(\mathbf{r},t_0+\Delta t)=\psi(\mathbf{r},t_0)$. We saw in the foregoing analysis that, effectively, only one screen is necessary. Consequently, we will also assume this fact and suppose that A_1 is the screen providing the smallest frequency cutoff. In this case the evolution of the wavefunction is given by

$$\psi'(\mathbf{r},t_1+\Delta t)=\int G(\mathbf{r},t_1+\Delta t;\mathbf{r}',t_2+\Delta t)A_1(r')\times G(\mathbf{r}',t_2+\Delta t;\mathbf{r}'',t_0+\Delta t)\times\psi'(\mathbf{r}'',t_0+\Delta t)\,\mathrm{d}^3r''\,\mathrm{d}^3r'. \tag{39}$$

In order to evaluate this expression we must substitute for the corresponding propagators, but expressed in terms of $u_1(t,t_0), u_2(t,t_0)$. We note that in this case neither $u_2(t_1+\Delta t, t_0)$ nor $u_1(t_1+\Delta t, t_0)$ and $\dot{u}_1(t_1+\Delta t, t_0)$ vanish so the resulting expressions are more involved compared to the proceeding case. Let us assume that Δt is small and derive an expression in this limit. The resulting algebra is somewhat lengthy but straightforward, so we write the final result for the Fourier transform of Eq. (39) i.e.,

$$\tilde{\psi}(\mathbf{k}, t_1+\Delta t) = \frac{1}{u_1(t_1)} A\left(\frac{\hbar}{m} u_2(t_1)u_1(t_2)k\right). \tilde{\psi}\left(u_2(t)R^{-1}\left(\frac{\theta(t_1,t_0)}{2}\right)\mathbf{k}, t_0+\Delta t\right) \times \exp\left\{\frac{\mathrm{i}\hbar}{2m}(u_2^2(t_1)-1)\Delta t k^2\right\} + \cdots \tag{40}$$

with $\tilde{\psi}(\mathbf{k}, t_1+\Delta t)$ and $\tilde{\psi}(\mathbf{k}, t_0+\Delta t)$ being, respectively, the Fourier transform of the image and object wavefunctions. In this expression we have deleted terms of higher order in Δt. Clearly this result reduces to Eq. (38) in the limit $\Delta t = 0$. We note that in this case the linear filter of the Fourier transformed object wave function is modified by a phase factor linear in Δt.

If we assume that the object wavefunction has the form given by Eq. (36) and construct the corresponding contrast function, the resulting expression becomes

$$\begin{aligned} 1 - u_2^2(t_1)|\psi(\mathbf{r}, t_1+\Delta t)|^2 &= 2\int \mathrm{e}^{\mathrm{i}\mathbf{kr}} \tilde{a}\left(u_2(t_1)R^{-1}\left(\frac{\theta(t_1,t_0)}{2}\right)\mathbf{k}\right) \\ &\quad \times A\left(\frac{\hbar}{m}u_1(t_2)u_2(t_1)k\right)\cos\left(\frac{\hbar}{2m}(u_2^2(t_1)-1)\Delta t k^2\right) \\ &\quad - 2\int \mathrm{e}^{\mathrm{i}\mathbf{kr}} \tilde{\sigma}\left(u_2(t_1)R^{-1}\left(\frac{\theta(t_1,t_0)}{2}\right)\mathbf{k}\right) \\ &\quad \times A\left(\frac{\hbar}{m}u_1(t_2)u_2(t_1)k\right) \\ &\quad \times \sin\left(\frac{\hbar}{2m}(u_2^2(t_1)-1)\Delta t k^2\right). \end{aligned} \tag{41}$$

Finally, if we Fourier transform this expression, we conclude that the image contrast is a linear combination of the spectrum of $\tilde{a}$ and $\tilde{\sigma}$, weighted by the lens amplitude and phase contrast functions

$$2\cos\left(\frac{\hbar}{2m}(u_2^2(t_1)-1)\Delta t k^2\right), \quad 2\sin\left(\frac{\hbar}{2m}(u_2^2(t_1)-1)\Delta t k^2\right) \tag{42}$$

and modulated by the screen aperture function. This completes our calculation and some comments are in order. In the first place, we note that these results are valid for bright field image formation produced by a coherent electron beam incident perpendicularly to the specimen. We also note that the effect of the finite electron pulse duration Δt produces phase contrast. This effect is similar to defocusing introduced in conventional static field lenses by displacing the screen aperture away from the diffraction plane so as to enhance contrast. The most significant difference with our case is the presence of the spherical aberration term.

In summary, we have analyzed the aberrations affecting image formation of a time dependent magnetic field lens, resulting from the time dependence of the system cardinal elements, the energy dispersion of the beam and diffraction. We have studied the conditions for which the former two effects can be reduced or eliminated by proper introduction of screens with apertures along the beam optical axis and adjustment of the magnetic field time dependence. As a result of this analysis we obtained the conditions for stationary images and derived the effect of diffraction in terms of contrast functions.

This work was supported by FONDECYT-CHILE Grant number 1010395 and Millennium Science Nucleus, Condensed Matter Physics P99-135-F.

Appendix

In order to justify the quasistatic approximation for the time dependent magnetic field inside the ellipsoidal coil, let us analyze a similar but mathematically simpler case of an infinite cylindrical coil having n turns per unit length. For a purely sinusoidal current, $I_0 \cos \Omega t$, where Ω and I_0 are arbitrary, the exact steady-state solution for the magnetic field is

$$B(r, t) = B_0 J_0(r\Omega/c) \cos \Omega t \hat{z},$$

where J_0 is the zero-order Bessel function and $B_0 = 4\pi n I_0/c$. If we analyze the field inside a tubular region concentric with the coil axis and having a diameter of, say, 1 cm and for the case of $\Omega \sim 10^8$, we derive that the maximal deviation due to the quasistatic approximation occurs at the boundary and is given by

$$\frac{B_{\text{quasistatic}} - B_{\text{exact}}}{B_{\text{exact}}} = I - J_0\left(\frac{0.5 \times 10^8}{3 \times 10^{10}}\right) \simeq 0.8 \times 10^{-4},$$

so less that 1/10000 for frequencies in the Ghz range. Obviously, for smaller Ω the smaller the effect is. In the case of a pulsed current, such as described in this work, we can easily extend our analysis by Fourier decomposing the current and apply the above result to each component. The validity of this approach is guaranteed by the superposition principle. In order to estimate the range of frequencies involved in the pulse, $\Delta\Omega$, let us assume it has a duration T so that $\Delta\Omega \sim 1/T$. As explained in the Refs. [5,6,8], the choice of T will depend on the time of transit of the electrons through the coil. This, in turn, will be a function of the coil length and the electrons incident energy. In principle, we can make T as long as we want by making the coil sufficiently long. (Reducing the electrons incident energy has the undesirable effect of increasing chromatic aberration.) In this way, we can reduce $\Delta\Omega$ accordingly. For illustrative purposes we have chosen the coil length ~ 1 m, $B_0 \sim 10^2 \sim 10^3$ G, so that the image amplification is $\sim 10^5$ and the electron energy ~ 1 keV. For these values $\Delta\Omega \sim 10^8$. Consequently, as long as electrons remain inside the tubular region indicated above, the quasistatic approximation is well justified.

References

[1] O. Scherzer, J. Appl. Phys. 20 (1949) 20.
[2] A. Septier, Adv. Opt. Electron Microsc. 1 (1966) 204.
[3] A. Crewe, H. Rose, in: Proceeding of Microscopy and Microanalysis 2002; Micros. Microanal. 8 (Suppl. 2) (2002) pp. 4,6.
[4] P. Hawkes, E. Kasper, Principles of Electron Optics, Vol. 2, Academic Press, England, 1966, pp. 872.
[5] M. Calvo, P. Lazcano, Optik 113 (2002) 31.
[6] M. Calvo, D. Laroze, Optik 113 (2002) 429.
[7] P. Hawkes, A. Kasper, Principles of Electron Optics, Vol. 3, Academic Press, London, 1994.
[8] M. Calvo, Optik 113 (2002) 233.